Characterization of a Photon Counting Test Bed for Space to Ground Optical Pulse Position Modulation Communications Links

Jennifer M. Nappier, Brian E. Vyhnalek, Sarah A. Tedder, and Nicholas C. Lantz
NASA Glenn Research Center 21000 Brookpark Road, Cleveland, Ohio 44135

ABSTRACT

The National Aeronautics and Space Administration (NASA) Glenn Research Center (GRC) has developed a laboratory transmitter and receiver prototype of a space-to-ground optical communications link. The system is meant to emulate future deep space optical communication links, such as the first crewed flight of Orion, in which the transmitted laser is modulated using pulse position modulation and the receiver is capable of detecting single photons. The transmitter prototype consists of a software defined radio, a high extinction ratio electro-optic modulator system, and a 1550 nm laser. The receiver is a scalable concept and utilizes a single-pixel array of fiber coupled superconducting nanowire single photon detectors. The transmit and receive waveforms follow the Consultative Committee for Space Data Systems (CCSDS) Optical Communications Coding and Synchronization Standard. A software model of the optical transmitter and receiver has also been implemented to predict performance of the optical test bed. This paper describes the transmitter and receiver prototypes as well as the system test configuration. System level tests results are presented and shown to align with predictions from software simulations. The validated software model can be used to in the future to reduce the design cycle of optical communications systems.

Keywords: Optical communications, software defined radio, pulse position modulation, waveform

1. INTRODUCTION

NASA communication systems are being upgraded in order to accommodate the increased data return requirements of future NASA missions. In the past, X-band or S-band links were capable of meeting the mission requirements for telemetry, tracking, and command (TT&C) as well as data return. In the future, missions will need a high data return communications link, and optical communications systems offer the benefit of high data return combined with lower mass and power than traditional radio frequency (RF) communications systems. NASA has already successfully demonstrated a 622 Mbps data rate with the Lunar Laser Communications Demonstration[1] (LLCD) in 2013. There are also several other upcoming NASA missions utilizing optical communications, including the Laser Relay Communications Demonstration[2] (LCRD), the Orion EM-2 Optical Communication Demonstration[3] (O2O), and the Psyche[4] mission to deep space. All of these missions utilize photon counting-based ground receiver systems and implement serially concatenated pulse position modulation (SCPPM)[5], the modulation upon which the Consultative Committee for Space Data Systems (CCSDS) Optical Communications Coding and Synchronization Red Book[6] standard is based.

An optical communications photon counting test bed has been implemented to enable development of a real time optical receiver system, which includes the aft optics, single photon counting detectors, and a real time field programmable gate array (FPGA) based receiver. The communications waveform implemented in the test bed conforms to the CCSDS Optical Coding and Synchronization telemetry link. A software Matlab model of the optical test bed has also been developed to model key sources of performance loss in the test bed. This paper describes the photon counting transmitter and receiver test bed, the software simulations, and system test results. The optical test bed is described in Section 2. Bit error rate (BER) software simulations used to predict performance of the test bed are described in Section 3. Section 4 shows the system test bed results align with the simulation results.

2. SYSTEM TEST BED DESCRIPTION

The optical test bed is designed to emulate the transmitter and receiver of photon counting optical communications links. A block diagram of the system is shown in Figure 1. A description of the optical transmitter, link emulation, and optical receiver follows.

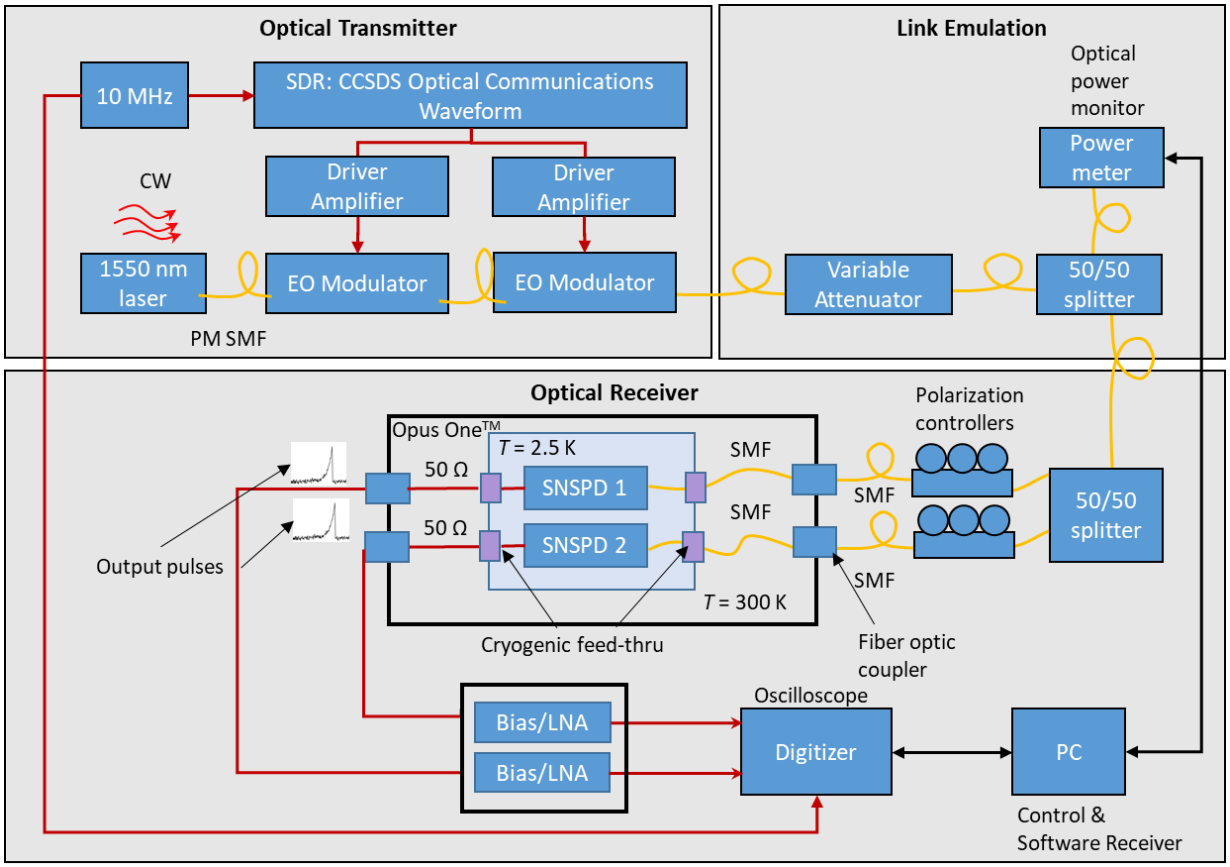

Figure 1. Block diagram of the optical communications system test bed.

2.1 Optical Transmitter

The optical transmitter consists of a software defined radio (SDR) running the optical waveform and a cascaded electro-optic (EO) modulator setup[7], which modulates a continuous wave laser with the electrical pulse output from the SDR.

The SDR consists of a Harris Corporation Reconfigurable Space Processor (RSP) development card and a custom optical mezzanine card[8]. The RSP contains two Xilinx Virtex 7 FPGAs, a digital signal processor (DSP), and supplemental memory. The RSP is controlled with a computer through the SpaceWire interface. The custom optical mezzanine card was developed at NASA Glenn Research Center (GRC). The optical mezzanine card performs serialization of the waveform signal which is sent out in parallel from the FPGA to the optical mezzanine card. The optical mezzanine card can generate a 2 GHz slot clock or can accept a slot clock from an external source. It divides the slot clock by 16 and sends it to the FPGA. The FPGA sends 16 parallel data lines to the optical mezzanine card, which then converts them into a serial stream. This serial data interfaces to the cascaded electro-optic modulator setup.

The optical waveform is targeted to one of the Xilinx Virtex 7 FPGAs on the Harris RSP. The waveform implements the CCSDS Optical Communications Coding and Synchronization Red Book High Photon Efficiency telemetry link[6]. This includes modulation orders M = 4, 8, 16, 32, 64, 128, and 256; and code rates 1/3, 1/2, and 2/3. Pseudorandom bit stream (PRBS) data is generated on the platform as a part of this waveform. The channel interleaver is implemented in the waveform, but has been bypassed for system testing. The waveform combined with the optical mezzanine card can generate PPM slot widths from 0.5 ns to 512 ns. A diagram of the optical waveform is shown in Figure 2.

The EO modulator system consists of two high extinction ratio EO modulators cascaded in series. The electrical PPM signal driving the modulators is offset in time so that the output optical PPM signal is narrowed. This pulse narrowing improves the extinction ratio[7].

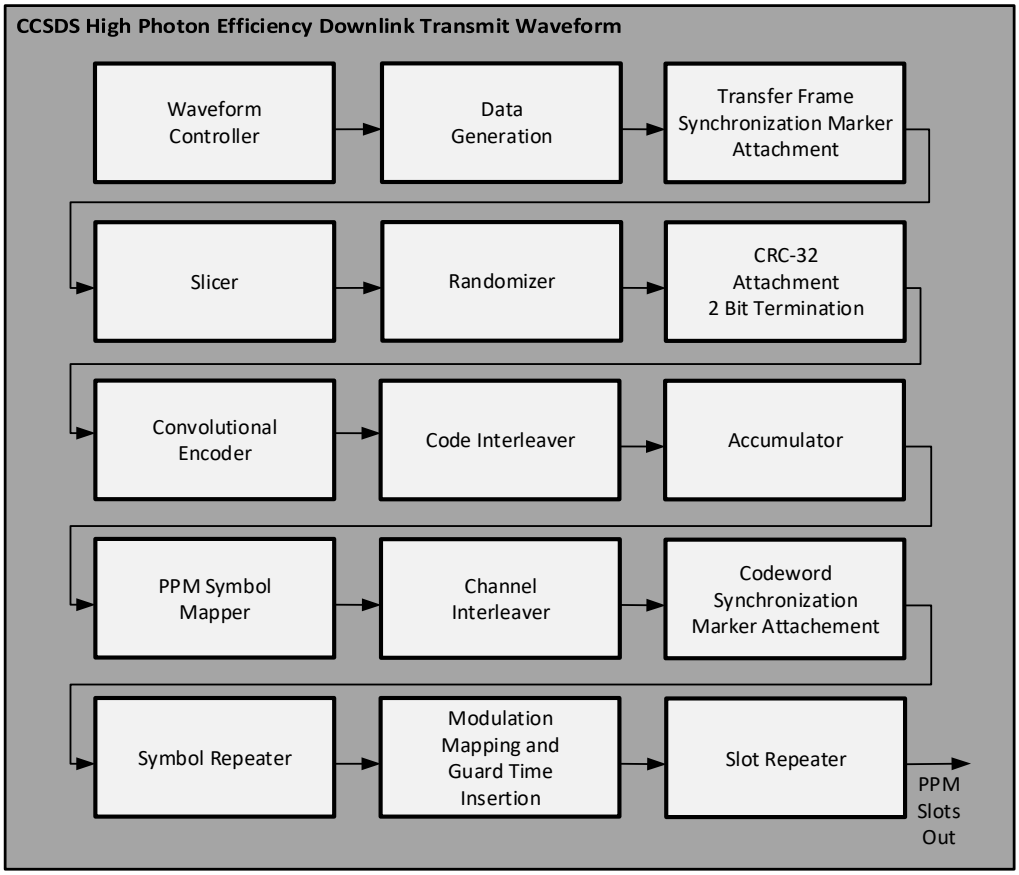

Figure 2. Transmit waveform block diagram.

2.2 Link Emulation

The photon counting optical communications link free space loss is emulated with a fiber digital variable attenuator. No noise is inserted and so the attenuator is used to change the signal power going into the receiver. A 50/50 fiber splitter is used to provide a test port for measuring optical power with a power meter, which is controlled by a computer.

2.3 Optical Receiver

The photon counting optical receiver consists of a 50/50 fiber splitter, fiber polarization controllers for each detector channel, two Quantum Opus superconducting nanowire single photon detectors (SNSPDs), detector bias and amplification, a digitizer, and a software model of the optical receive waveform.

The attenuated signal from the optical transmitter is split so that the two detectors can receive the transmitted signal simultaneously. The detection efficiency of the Quantum Opus detectors is dependent on the polarization of the incoming signal. The polarization controllers are used to maximize the photon counts out of the detectors by optimizing the polarization alignment.

Two single mode fiber coupled detectors from the Quantum Opus, LLC Opus One™ system are used in the receiver. The Opus One™ operates at a temperature of 2.5 K using a closed-cycle helium water-cooled cryocooler housed in a 3U 19-inch rack-mountable unit. The nanowire detectors are optimized for 1550 nm operating wavelength. Electrically the devices are current biased with adjustable front panel controls, and coupled to 50 Ω coaxial readout cables to room temperature amplifiers with 500 MHz bandwidth and a maximum 55.6 dB gain. Detector performance metrics of jitter, efficiency, and blocking are relevant to system testing.

The detector system jitter as a function of bias current was characterized[9]. Results are shown in Figure 3. For system testing, detector channel 1 is biased at 10.5 µA and channel 2 is biased at 9.8 µA. This gives the full width at half maximum (FWHM) detector jitter for channel 1 of 68 ps and channel 2 of 85 ps.

The maximum system detection efficiency at optimal polarization was also characterized as shown in the Figure 4. As the photon flux increases, the detection efficiency decreases due to detector blocking. The maximum blocking time on these detectors was measured to be 20 ps. As can be seen in the figure, at higher photon flux rates, the gap between the polarization-dependent detection efficiency becomes smaller. The detection efficiency range for these tests is between 50-60%.

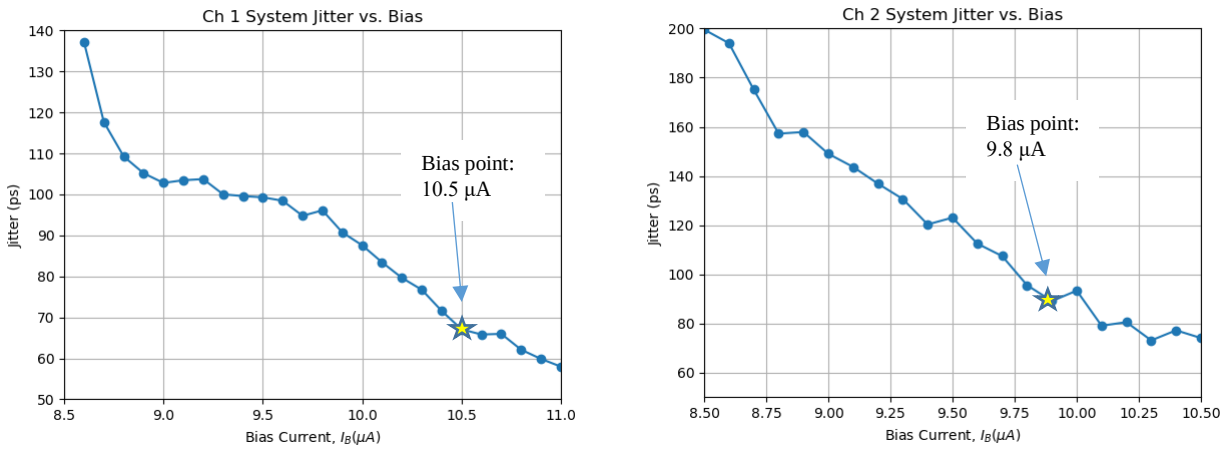

(a) (b)

Figure 3: FWHM jitter measurements for the quantum opus detectors channel 1 (a) and channel 2 (b).

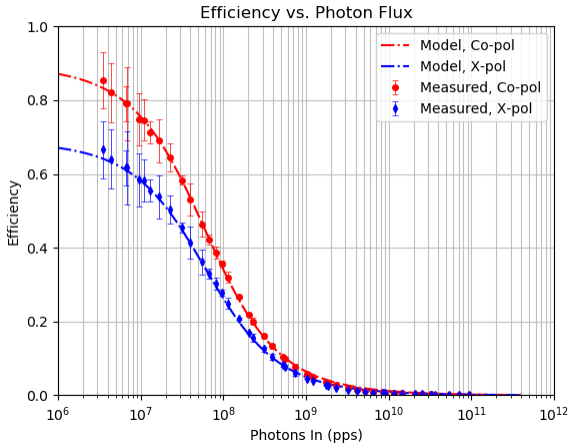

Figure 4. Polarization dependent detection efficiency with our operating range

An oscilloscope is used to digitize and save the pulses output from the SNSPDs. A computer is used to sample the detector pulses simultaneously with the power meter readings in order to verify the input power into the detectors is constant throughout the data capture. The clocks of the transmitter SDR and the receiver digitizer are locked for this test in order to eliminate error caused by clock recovery. The pulses are digitized at a rate of 2 GSps and post-processed using a Matlab receiver.

The Matlab receiver performs slot and symbol recovery[10]. Once the slot and symbol boundaries have been calculated, the receiver slot recovery algorithm delays and interpolates the incoming detector pulse samples. A threshold is used to find

the rising edge of the interpolated pulses and this data is down-sampled to count photon counts per slot. The rise time of the detector pulses is 850 ps and the pulses are sampled at a rate of 2 GHz. Since the sample rate does not meet the required Nyquist frequency, additional jitter of approximately 45 ps is introduced. The total jitter is 61 ps RMS for channel 1 and 68 ps RMS for channel 2. As a part of the slot and symbol recovery algorithm, the signal photon counts per signal slot (Ks) and the background photon counts per slot (Kb) are also calculated.

Once the symbol and slot boundaries are calculated, the receiver then performs code word alignment and calculates the log likehood ratios (LLRs) for each slot. SCPPM iterative decoding is completed using the Bahl, Cocke, Jelinek and Raviv (BCJR) algorithm. The decoded data is then de-randomized and de-sliced before the transfer frames are synchronized and a bit error rate on the PRBS data is calculated. A block diagram of the receiver Matlab model is shown in Figure 5.

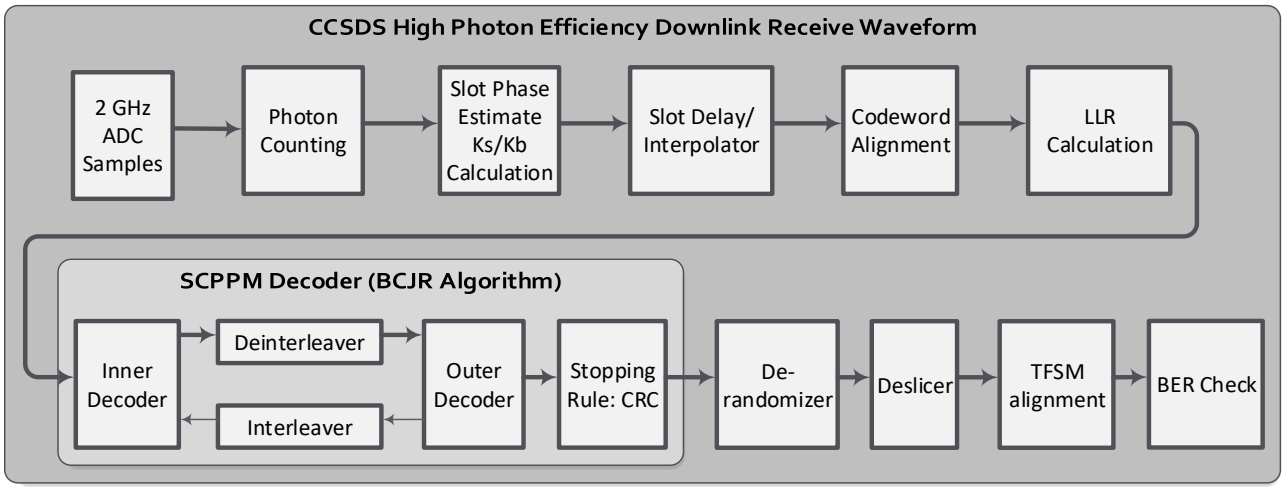

Figure 5. Block diagram of receive waveform model

3. SIMULATION RESULTS

Sources of error including jitter, detector blocking loss, and the number of detectors used can impact the performance of the system. Bit error rate (BER) curve floating point simulations were performed using a Matlab model of the transmit and receive waveform. The waveform selected was the PPM-32, code rate 1/3 waveform. The background photon counts per slot (Kb) were Kb=0.0001. The signal photon counts (Ks) were varied to produce the BER curve. Each data point was simulated using 1,000 code words. The slot width, total system jitter, number of detectors, and detector blocking were varied. The test cases are listed in Table 1.

In the first simulation, the number of detected photons is equal to the number generated by the Poisson distribution. In the second simulation, the Poisson distribution was used to generate detected photons, but the number of detectors was limited to 1. The third simulation again limits the number of detectors to 1, but also adds detector blocking of 20 ns. It is at this point that the slot width of 1 ns is introduced. The previous simulations were independent of the slot width. The fourth simulation includes 1 detector, 20 ns of detector blocking, a 1 ns slot, and 80 ps of system jitter. An ADC sample rate of 2 GHz is also introduced. In order to add jitter, the detected photons are first placed within the slot using a uniform distribution, and then the system jitter is added with a normal distribution. The fifth simulation is the same as the previous except with 60 ps of system jitter.

The simulation results are presented in Figure 6. The baseline simulation with the number of detectors as generated in the Poisson distribution is shown in the purple squares. The capacity curve was generated using a Monte Carlo method and is represented by the grey dots. When the number of detectors is limited to 1, the BER curve (navy blue triangles) shifts significantly to the left from the baseline floating point simulation so that it is very close to the capacity curve. This shift is possible in this case due to the very low noise in the system simulation (Kb=0.0001). When there is no background noise in a symbol, it does not matter if 3 photons have been detected or 1 photon has been detected in a slot; the symbol will

decode correctly. Therefore, the BER curve shifts to the left. It can be seen that adding detector blocking of 20 ps (light blue circles) does not have a significant effect on the performance of the waveform selected. However, the addition of the 60 or 80 ps RMS of system jitter shifts the curve back to the right. The addition of 60 ps RMS jitter causes a 0.6 dB performance loss and the addition of 80 ps RMS jitter causes a 0.8 dB loss.

Table 1. Simulations settings for the PPM-32, Code Rate 1/3, Kb=0.0001 photons/slot waveform

Simulation	Slot Width (ns)	ADC Sample Rate (GHz)	Number of Detectors	Detector blocking (ns)	System Jitter (ps RMS)
1: n detectors	-	-	As generated by Poisson distribution	0	0
2: 1 detector	-	-	1	0	0
3: 1 detector; 20 ns blocking	1	-	1	20	0
4: 1 detector; 20 ns blocking ;80 ps RMS jitter	1	2	1	20	80
5: 1 detector; 20 ns blocking; 60 ps RMS jitter	1	2	1	20	60

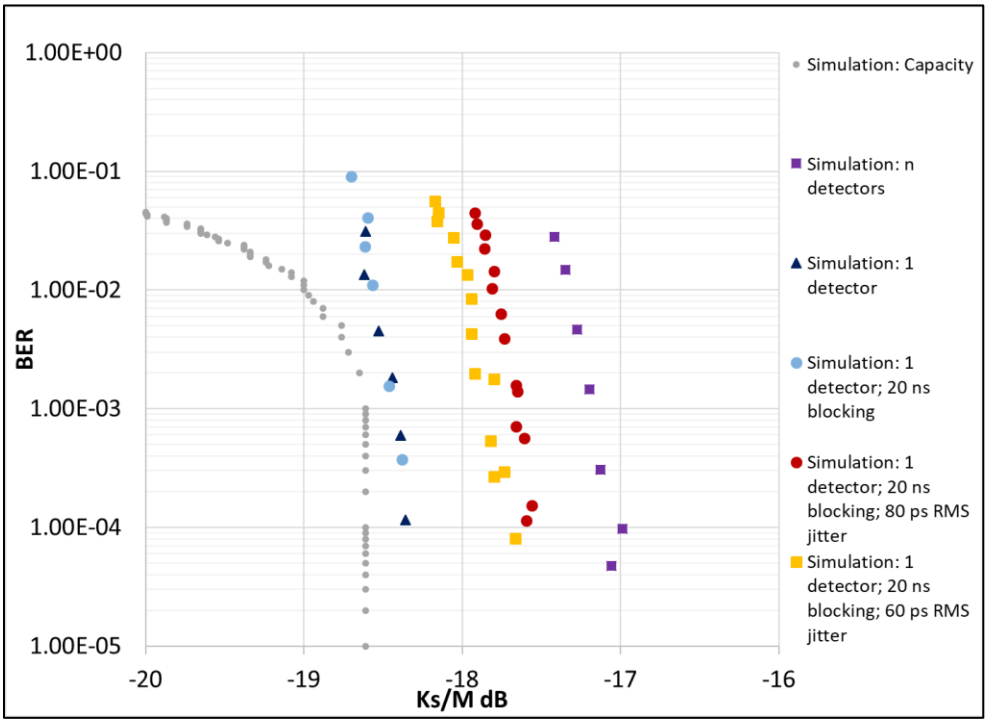

Figure 6. BER curve simulation results from the PPM-32, slot width 1 ns, code rate 1/3 waveform; Kb=0.0001

4. SYSTEM TESTING RESULTS

System testing was conducted using the optical transmitter and receiver system test setup described in Section 2. The waveform selected was the PPM-32, code rate 1/3, slot width 1 ns, 40 Mbps waveform. This waveform was selected because it is the lowest PPM order and smallest slot width that a single detector could successfully receive error free. The detector blocking time of 20 ns was shown to have a low impact on the performance of this waveform in Section 3. BER curve results from the system testing are presented Figure 7. The results from the 60 ps and 80 ps RMS jitter simulations are also included in the figure. As can be seen in the graph, detector channel 1 (green triangles) is slightly to the left of detector channel 2 (blue diamonds). Detector 1 has less jitter than detector 2, and so it performs slightly better. The detector channel 1 (61 ps RMS jitter) results are on top of the 60 ps RMS jitter simulation curve and the detector channel 2 (68 ps RMS jitter) results are on top of the 80 ps RMS jitter simulation curve. The system predicted jitter values of 61 and 68 ps RMS match very closely to the simulation results and the system test results.

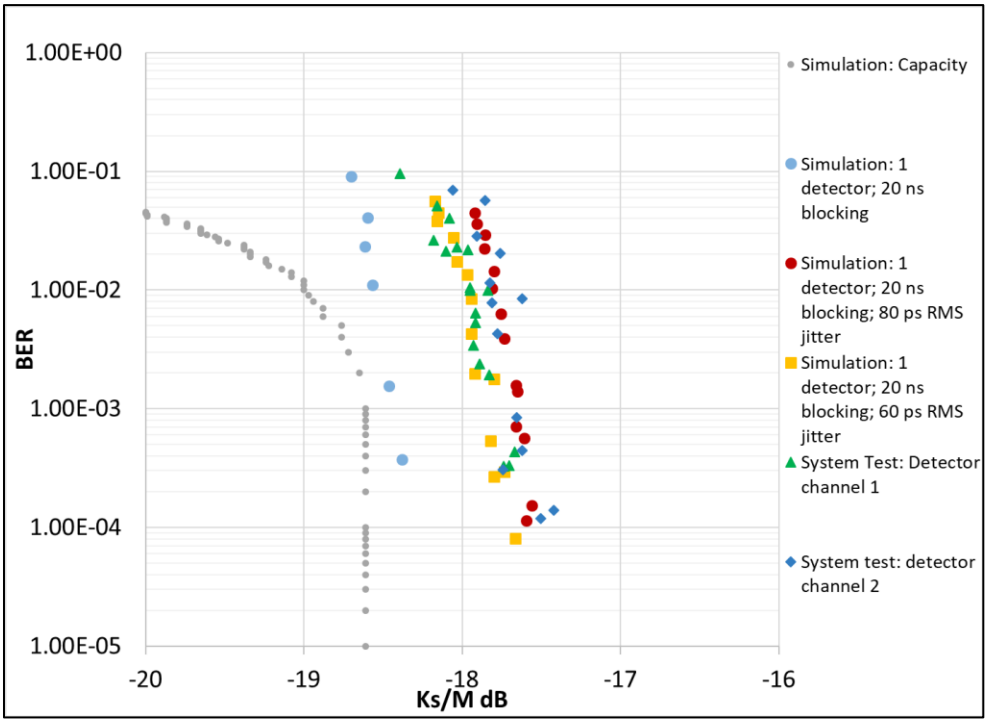

Figure 7. System testing BER curve results from the PPM-32, slot width 1 ns, code rate 1/3 waveform; Kb=0.0001

5. CONCLUSIONS

A photon counting optical communications system test bed was designed and characterized. The test bed includes an optical transmitter and photon counting receiver compatible with the CCSDS Optical Communications Coding and Synchronization Red Book telemetry link. Key parameters of the system were modeled in simulations including background noise, number of detectors used, detector jitter, and detector blocking. The BER curve results for the system test bed align with the simulation results. Therefore, sources of loss in the system have been accurately characterized and the model can be used to predict performance of other communications waveforms. The model can be used in the future to design other optical PPM communications systems without the need to prototype them in a test bed, reducing the design cycle.

6. ACKNOWLEDGEMENTS

This work was performed under the NASA Space Communications and Navigation Program at the NASA Glenn Research Center.

REFERENCES

[1] Boroson, D., Robinson, S. Murphy, D., Khatri, F., Kovalik, J., Sodnik, Z., and Cornwell, D. "Overview and Results of the Lunar Laser Communication Demonstration," Proc. SPIE Free-Space Laser Communication and Atmospheric Propagation XXVI 8971 (2014)

[2] Edwards, B., Israel, D., and Vithlani, S. "Latest Changes to NASA's Laser Communications Relay Demonstration Project," Proc. SPIE Free-Space Laser Communication and Atmospheric Propagation XXX 10524 (2018)

[3] Robinson, B., Shih, T., Khatri, F., Boroson, D., Burnside, J., Guldner, O., Constantine, S., Torres, J., Yarnall, T., DeVoe, C., Hubbard, W., Geisler, D., Stevens, M., Mikulina, O., Spellmeyer, N., Wang, J., Butler, R., Hogan, M., King, T., and Seas, A. "Laser Communications For Human Space Exploration in Cislunar Space: ILLUMA-T and O2O," Proc. SPIE Free-Space Laser Communication and Atmospheric Propagation XXX 10524 (2018)

[4] Biswas, A., Srinivasan, M., Piazzolla, S., and Hoppe, D. "Deep Space Optical Communications," Proc. SPIE Free-Space Laser Communication and Atmospheric Propagation XXX 10524 (2018)

[5] Moison, B. and Hamkins, J., "Coded Modulation for the Deep-Space Optical Channel: Serially Concatenated Pulse Position Modulation," The Interplanetary Network Progress Report 42(161) (2005).

[6] "Optical Communications Coding and Synchronization Draft Recommended Standard," CCSDS 142.0-R-1 Red Book (2018).

[7] Lantz, N., Nappier, J., Vyhnalek, B. and Tedder, S. "Optical Software Defined Radio Transmitter Extinction Ratio Enhancement with Differential Pulse Carving," Proc. SPIE Free-Space Laser Communication and Atmospheric Propagation XXXI 10910 (62) 2019.

[8] Nappier, J. and Lantz, N. "Development of an Optical Slice for an RF and Optical Software Defined Radio," Proc. SPIE Free-Space Laser Communication and Atmospheric Propagation XXX 10524 (51) 2018.

[9] Vyhnalek, B., Tedder, S., Katz, E., and Nappier, J. "Few-mode Fiber Coupled Superconducting Nanowire Single-Photon Detectors for Photon Efficient Optical Communications," Proc. SPIE Free-Space Laser Communication and Atmospheric Propagation XXXI 10910 (11) (2019).

[10] Rogalin, R. and Srinivasan, M. "Synchronization for Optical PPM with Inter-Symbol Guard Times," The Interplanetary Network Progress Report 42(209) (2017).